



Study of the non-Newtonian behaviour of Reiner Rivlin relative to power law in arterial stenosis

Nibedita Dash* and Sarita Singh

Department of Mathematics, School of Physical Sciences, Doon University, Dehradun, India.

Abstract

The present paper develops the solution of steady axi-symmetric Navier-Stokes conservation equations incorporating Reiner Rivlin stress and strain rate relation that represents generalized non-Newtonian fluid. Perturbation solution is obtained to determine the flow field for axially symmetric stenosed artery. The flow field obtained from the Perturbation solution is compared with the exact analytical solution. In perturbation solution, cross viscosity that represents non-Newtonian characteristics is considered a perturbation parameter, and the result obtained is observed to be dependent on the perturbation parameter. At smaller values of cross viscosity, the perturbation result is significantly closer to the analytical solution. But, as the values of cross viscosity increase, the perturbation results show a wider deviation from analytical results. Further, in this paper, the results of Reiner Rivlin are compared with the results obtained from the Power Law stress and strain rate relation. Such comparison of results of Reiner Rivlin with Power law is utilized to study the flow characteristics of blood. The flow profile in the case of Reiner Rivlin is observed to be significantly closer to that of Power law. The study infers that Reiner Rivlin's constitutive relation is fairly suitable in simulating blood flow in arterial stenosis.

Keywords. Stenosis, Reiner-Rivlin fluid, Viscosity, Cross viscosity, Perturbation.

2010 Mathematics Subject Classification. 35B20, 35Q35.

1. INTRODUCTION

Arterial stenosis is due to the gradual constriction of an artery by the accumulation of cholesterol, calcium and other fatty substances [25]. The arterial blood flow is subjected to increased resistance leading to hypertension and triggers significant deviation in characteristics of blood flow such as velocity profile, axial pressure distribution, shear stress at the wall, and resistance impedance. One of the established approaches is to correlate the altered blood flow characteristics with the degree of obstruction in stenosis. But concurrently, the flow characteristics are greatly influenced by blood rheology, which is highly complex. A set of factors such as viscosity of plasma, rate of shear, degree of aggregation of red blood cells, and deformability of bi-concave erythrocytes, percentage of haematocrit is reported to significantly affect shear stress and viscosity of blood [6, 20, 26]. Blood viscosity depends on arterial diameter. Such dependency called Fahraeus and Lindquist effect is further significant in stenosis as it constricts the artery reducing its size. Blood by composition is a heterogeneous suspension of deformable cells in watery plasma. The rheological behavior is governed by the compositions of blood and their mutual interactions and interactions with the surrounding structures. While the flow of plasma exhibits Newtonian characteristics, whole blood is non-Newtonian in nature as RBC occupies around 40-46 percent of volume in the blood and contributes to the increase in viscosity.

Viscosity is the most dominant factor that influences blood flow characteristics. In the large diameter of the blood vessels, at high shear rate blood may maintain constant viscosity but as it becomes smaller, the influence of cells, RBC in particular, becomes predominant to induce a low shear rate. As per a report, viscosity and viscoelasticity are increased due to the hardening of the erythrocytes [21]. Change in viscoelasticity behavior is influenced at higher shear rates causing dilatancy.

Received: 30 July 2021 ; Accepted: 19 April 2022.

* Corresponding author. Email: dashnibedita@yahoo.co.in .

From the literature [22], it is well established that to account for non-constant viscosity of blood, various constitutive relations where viscosity is considered to be either dependent on shear rate or stress are developed. Power Law is found to be the most widely considered as it fits well with the experimental data. These models satisfactorily consider shear-thinning viscosity, and yield stress, but are not suitable for the dilatancy effect. In order to predict dilatancy in wet sand, Massoudi [11] has developed a different type model using generalized Reiner Rivlin constitutive relation. In such a case, shear viscosity depends on both shear rate and volume fraction in suspension. Considering the fact that blood shows both shear thinning and thickening properties as shear increases due to Fahraeus and Lindquist effect and dilatancy effect due to suspension nature, the use of Reiner-Rivlin constitutive relation seems to be appropriate in modeling blood flow in the stenosed artery. Therefore, in the present paper, conservation equations are formulated considering Reiner-Rivlin constitutive relation. The expression for flow field is obtained for axi-symmetric case considering axially symmetric stenosis. The differential type Reiner Rivlin constitutive relations render the conservation equations non-linear. Considering non linearity of governing equations, an attempt has been made to develop a solution for the flow field by applying the Perturbation method. The results obtained in terms of the flow field are compared with the analytical method.

To account for variable viscosity, shear rate dependent viscous inelastic constitutive models are reported in the literature. Literature is rich where in the Power-law [17, 18], H-B [1, 14, 24], the Casson [5, 10, 19, 23] and the Carreau fluids [2, 4, 15] are considered. Power-law considers variable viscosity dependent on strain rate and analytical results are available in describing the arterial blood flow situation. Viscosity and shear rate in Power law exhibits a linear relationship on a logarithmic scale. Similarly, the attempt of researchers in measuring the viscosity of blood by using either a falling-ball viscometer or a cone-plate viscometer for a range of shear rate from 0.1 to 400 s⁻¹ is responding yield straight line [8]. Therefore, it can be inferred that the power-law model to acceptable precision provides the best fit with the experimental data [8, 23]. Apart from strain rate dependent viscosity, the non-Newtonian character of blood is due to yield stress [9]. Casson fluid constitutive relation is used as visco-inelastic non-Newtonian fluid with yield stress. This fact has motivated the present study to compare the results obtained from Reiner Rivlin with the results obtained from Power-law and Casson constitutive relations. Such comparison is intended to establish the non-Newtonian character of Reiner Rivlin relative to shear rate dependent non-Newtonian fluid without or with yield stress.

Therefore, the conservation equations are solved using both Power-law and Casson constitutive relations using the same conditions in which Reiner Rivlin is solved. Such an approach is expected to establish the efficacy of Reiner Rivlin's constitutive relation in modeling the flow of blood in the stenosed arteries.

2. FORMULATION OF PROBLEM:

The present paper attempts to solve Navier-Stokes equations for momenta and mass for axis-symmetric case considering constitutive relations for both Reiner Rivlin fluid, and Power Law. The solution is obtained by considering following conditions.

- (1) Cylindrical co-ordinate (r, z) is considered with r= 0 is the axis of symmetry of artery,
- (2) Incompressible flow of blood in artery is considered.
- (3) Steady flow of blood is considered.
- (4) Viscosity is considered to be constant.
- (5) Density of blood is assumed to be constant.

Considering above conditions, the conservation equations of mass and momentum in dimensional form are:

$$\frac{\partial \bar{u}}{\partial \bar{r}} + \frac{\bar{u}}{\bar{r}} + \frac{\partial \bar{w}}{\partial \bar{z}} = 0, \tag{2.1}$$

$$\rho \left(\bar{u} \frac{\partial \bar{u}}{\partial \bar{r}} + \bar{w} \frac{\partial \bar{u}}{\partial \bar{z}} \right) = \frac{1}{\bar{r}} \frac{\partial}{\partial \bar{r}} (\bar{r} \bar{\tau}_{\bar{r}\bar{r}}) + \frac{\partial \bar{\tau}_{\bar{z}\bar{r}}}{\partial \bar{z}} - \frac{\bar{\tau}_{\bar{\theta}\bar{\theta}}}{\bar{r}}, \tag{2.2}$$

$$\rho \left(\bar{u} \frac{\partial \bar{w}}{\partial \bar{r}} + \bar{w} \frac{\partial \bar{w}}{\partial \bar{z}} \right) = \frac{1}{\bar{r}} \frac{\partial}{\partial \bar{r}} (\bar{r} \bar{\tau}_{\bar{z}\bar{r}}) + \frac{\partial \bar{\tau}_{\bar{z}\bar{z}}}{\partial \bar{z}}. \tag{2.3}$$



The schematic diagram of stenotic artery with co-ordinate system is shown in Figure 7.

Let the following non-dimensional variables are introduced.

$$\bar{r} = rd_0; \bar{z} = bz; \bar{w} = u_0w; \bar{u} = \left(\frac{u_0\delta}{b}\right)u; \bar{p} = \left(\frac{u_0b\mu}{d_0^2}\right)p; \bar{h} = d_0h; Re = \frac{\rho bu_0}{\mu}; \gamma = \frac{\mu_c u_0}{\mu b}$$

$$\bar{\tau}_{\bar{r}\bar{r}} = \left(\frac{b}{u_0\mu}\right)\tau_{\bar{r}\bar{r}}; \bar{\tau}_{\bar{z}\bar{r}} = \left(\frac{d_0}{u_0\mu}\right)\tau_{\bar{z}\bar{r}}; \bar{\tau}_{\bar{z}\bar{z}} = \left(\frac{b}{u_0\mu}\right)\tau_{\bar{z}\bar{z}}; \bar{\tau}_{\bar{\theta}\bar{\theta}} = \left(\frac{b}{u_0\mu}\right)\tau_{\bar{\theta}\bar{\theta}}$$

Further, let the following conditions are considered for mild stenosis [3, 12].

$$\frac{\delta}{d_0} \ll 1; \frac{Re\delta n^{\left(\frac{1}{n-1}\right)}}{b} \ll 1; \frac{d_0 n^{\left(\frac{1}{n-1}\right)}}{b} \sim 0.$$

The equations governing steady flow of incompressible fluid in cylindrical coordinate in non-dimensional form reduce to:

$$\frac{\partial u}{\partial r} + \frac{u}{r} + \frac{\partial w}{\partial z} = 0, \tag{2.4}$$

$$\frac{\partial p}{\partial r} = 0, \tag{2.5}$$

$$\frac{\partial p}{\partial z} = \frac{1}{r} \frac{\partial}{\partial r} (r\tau_{rz}). \tag{2.6}$$

The geometry of stenosis in non-dimensional form is mathematically described as [3, 12]

$$h_z = \begin{cases} d_z [1 - \omega \{(z - s) - (z - s)^n\}], & s \leq z \leq 1 + s \\ d_z, & \text{otherwise, } d_z = 1 + \varphi z \end{cases} \tag{2.7}$$

Where $\omega = \frac{\delta(n)^{\frac{n}{n-1}}}{(n-1)d_0b^n}$, $s = \frac{a}{b}$, n is shape factor and $\varphi = \tan \tilde{\theta}$.

For non-tapered artery, $\tilde{\theta} = 0$, divergent artery, $\tilde{\theta} \geq 0$ and convergent artery, $\tilde{\theta} \leq 0$.

The wall shear stress is evaluated from Equation (2.6). Integrating Equation (2.6) with respect to r , the wall shear stress τ_w is evaluated from τ_{rz} at $r = h_z$.

The wall shear stress becomes:

$$\tau_w = \frac{1}{2} \frac{\partial p}{\partial z} h_z. \tag{2.8}$$

2.1. Constitutive equations for Reiner Rivlin fluid: Considering isotropic fluid, according to Reiner and Rivlin, the general relation between stress tensor τ_{ij} and rate of deformation ϵ_{ij} is given as [3, 8, 13]

$$\tau_{ij} = -p\hat{\delta}_{ij} + \mu_{ij}\epsilon_{ij} + \mu_c\epsilon_{ij},$$

where, strain rate tensor $\epsilon_{ij} = \epsilon_{ik}\epsilon_{kj}$, Kronecker delta ($\hat{\delta}_{ij}$). The value of $\hat{\delta}_{ij} = 0$ when $i = j$ and $\hat{\delta}_{ij} = 1$ when $i \neq j$. i may be either r or z or θ and j may also be either r or z or θ . Further, μ and μ_c are viscosity with dimension $[ML^{-1}T^{-1}]$ and cross viscosity with dimension $[ML^{-1}]$ respectively. μ_c is considered as a second order parameter of non-Newtonian fluid.

The stress tensors in cylindrical coordinates (r, z) in dimensional form is [3, 8, 13]:

$$\tau_{\bar{r}\bar{z}} = \mu \left(\frac{\partial \bar{u}}{\partial \bar{z}} + \frac{\partial \bar{w}}{\partial \bar{r}} \right) + 2\mu_c \left[\left(\frac{\partial \bar{u}}{\partial \bar{r}} \right) \left(\frac{\partial \bar{u}}{\partial \bar{z}} + \frac{\partial \bar{w}}{\partial \bar{r}} \right) + \left(\frac{\partial \bar{u}}{\partial \bar{z}} + \frac{\partial \bar{w}}{\partial \bar{r}} \right) \left(\frac{\partial \bar{w}}{\partial \bar{z}} \right) \right]. \tag{2.9}$$

Using non-dimensional variables introduced in section 2.1 in Equation (2.9), the expression for τ_{rz} is obtained. The same is substituted in Equation (2.6). Further, using mild stenosis conditions, Equation (2.6) reduces to:

$$\frac{\partial p}{\partial z} = \frac{1}{r} \frac{\partial}{\partial r} \left[r \frac{\partial w}{\partial r} + 2\beta r \frac{\partial w}{\partial r} \frac{\partial w}{\partial z} \right].$$



Therefore, after converting Equations (2.4), (2.5), and (2.6) to non-dimensional form and using mild stenosis conditions, the conservation equations in non-dimensional form non-dimensional form reduces to:

$$\frac{\partial u}{\partial r} + \frac{u}{r} + \frac{\partial w}{\partial z} = 0, \tag{2.10}$$

$$\frac{\partial p}{\partial r} = 0, \tag{2.11}$$

$$\frac{\partial p}{\partial z} = \frac{1}{r} \frac{\partial}{\partial r} \left[r \frac{\partial w}{\partial r} + 2\beta r \frac{\partial w}{\partial r} \frac{\partial w}{\partial z} \right]. \tag{2.12}$$

The initial and boundary conditions considered in the present study are:

$$\frac{\partial w}{\partial r} = 0 \text{ at } r = 0; w = 0 \text{ at } r = h_z \text{ and } u = \text{finite and constant}$$

2.2. Constitutive equations for Power Law fluid and Casson Fluid: The stress tensor for viscous fluid is given as: $\tau_{ij} = -\mu(\epsilon_{ij})\epsilon_{ij}$, where $\mu(\epsilon_{ij})$ is viscosity and $\epsilon_{ij} = -\frac{\partial w}{\partial r}$.

The constitutive equation for Power-law is expressed as [23, 24]:

$$\mu(\epsilon_{ij}) = m\epsilon_{ij}^{n-1},$$

where n is dimensionless flow index and consistency index m .

When $n < 1$, the fluid behaves as shear-thinning like blood, where in, viscosity decreases with the increase in shear rate. Similarly, when $n > 1$, fluid shows shear-thickening characteristics where in viscosity increases as shear rate increases. At $n = 1$ and m remains constant, the fluid behaves as Newtonian fluid. Therefore, the comparative study of flow field obtained from Reiner Rivlin Model and Power Law model for different n is expected to establish appropriateness of Reiner Rivlin model to mathematically represent the variable blood rheology at different metabolic and physical conditions highlighted in review of literatures.

Similarly, the constitutive equation for Casson fluid is expressed as [23, 24]:

$$(\tau_{rz})^{\frac{1}{2}} = \left(\mu \frac{\partial w}{\partial r}\right)^{\frac{1}{2}} + (\tau_0)^{\frac{1}{2}}, \tau_{rz} \geq \tau_0 \text{ and } \frac{\partial w}{\partial r} = 0, \tau_{rz} < \tau_0$$

3. SOLUTION OF REINER RIVLIN MODEL:

The conservation equation in non-dimensional form given in Equation (2.12) is a nonlinear partial differential equation. In the present paper, the solution is obtained by employing perturbation method. The result obtained from semi-analytical perturbation method is compared with exact solution reported by author in earlier paper.

To get the Perturbation solution, let Axial velocity (w), Pressure (p) and Flow rate (Q) are expanded considering β as the Perturbation parameter. The expanded expressions are:

$$w = w_0 + \beta w_1 + \beta^2 w_2 + \dots,$$

$$p = p_0 + \beta p_1 + \beta^2 p_2 + \dots,$$

$$Q = Q_0 + \beta Q_1 + \beta^2 Q_2 + \dots$$

Using above expansions in Equation (2.12), it becomes:

$$\begin{aligned} r \frac{1}{2} \left(\frac{\partial p_0}{\partial z} + \beta \frac{\partial p_1}{\partial z} + \beta^2 \frac{\partial p_2}{\partial z} + \dots \right) &= \left(\frac{\partial w_0}{\partial r} + \beta \frac{\partial w_1}{\partial r} + \beta^2 \frac{\partial w_2}{\partial r} + \dots \right) \\ &+ 2\beta \left(\frac{\partial w_0}{\partial r} + \beta \frac{\partial w_1}{\partial r} + \beta^2 \frac{\partial w_2}{\partial r} + \dots \right) \left(\frac{\partial w_0}{\partial z} + \beta \frac{\partial w_1}{\partial z} + \beta^2 \frac{\partial w_2}{\partial z} + \dots \right). \end{aligned}$$

Ignoring higher order of β , above equation becomes:

$$r \frac{1}{2} \left(\frac{\partial p_0}{\partial z} + \beta \frac{\partial p_1}{\partial z} \right) = \left(\frac{\partial w_0}{\partial r} + \beta \frac{\partial w_1}{\partial r} \right) + 2\beta \left[\left(\frac{\partial w_0}{\partial r} \frac{\partial w_0}{\partial z} + \beta^2 \frac{\partial w_1}{\partial r} \frac{\partial w_1}{\partial z} \right) \right]. \tag{3.1}$$



The zeroth order system becomes:

$$r \frac{1}{2} \left(\frac{\partial p_0}{\partial z} \right) = \left(\frac{\partial w_0}{\partial r} \right). \tag{3.2}$$

Integrating above equation with respect to r and using boundary condition, it becomes:

$$w_0 = \frac{\partial p_0}{\partial z} \left[\frac{r^2 - h_z^2}{4} \right]. \tag{3.3}$$

The first order system becomes:

$$r \frac{1}{2} \left(\frac{\partial p_1}{\partial z} \right) = \left(\frac{\partial w_1}{\partial r} \right) + 2 \left(\frac{\partial w_0}{\partial r} \frac{\partial w_0}{\partial z} \right). \tag{3.4}$$

Substituting w_0 and $\frac{\partial w_0}{\partial z}$, first order system Eq. (3.4) becomes:

$$r \frac{1}{2} \left(\frac{\partial p_1}{\partial z} \right) = \left(\frac{\partial w_1}{\partial r} \right) + 2r \frac{1}{2} \left(\frac{\partial p_0}{\partial z} \right) \left[\left(\frac{\partial^2 p_0}{\partial z^2} \left[\frac{r^2 - h_z^2}{4} \right] + \frac{\partial p_0}{\partial z} \left[\left(\frac{-h_z}{2} \right) \left(\frac{\partial h_z}{\partial z} \right) \right] \right) \right].$$

Integrating above equation with respect to r and using boundary condition: at $r = h_z, w_1 = 0$ it becomes:

$$w_1 = \frac{\partial p_1}{\partial z} \left[\frac{r^2}{4} - \frac{h_z^2}{4} \right] - \left(\frac{\partial p_0}{\partial z} \right) \left(\frac{\partial^2 p_0}{\partial z^2} \right) \left(\frac{r^4}{16} - \frac{r^2 h_z^2}{8} + \frac{h_z^4}{16} \right) + \left(\frac{\partial p_0}{\partial z} \right)^2 \left(h_z \frac{\partial h_z}{\partial z} \right) \left(\frac{r^2}{4} - \frac{h_z^2}{4} \right). \tag{3.5}$$

Using w_0 given in Eq. (3.1) and its derivative and w_1 in Eq. (3.5) and its derivative, the expression of w becomes:

$$w = \left(\frac{\partial p}{\partial z} \right) \left[\frac{r^2 - h_z^2}{4} \right] + \beta \left\{ \left(\frac{\partial p}{\partial z} \right)^2 \left(h_z \frac{\partial h_z}{\partial z} \right) \left(\frac{r^2}{4} - \frac{h_z^2}{4} \right) + \left(\frac{\partial p}{\partial z} \right) \left(\frac{\partial^2 p}{\partial z^2} \right) \left(\frac{r^2 h_z^2}{8} - \frac{r^4}{16} - \frac{h_z^4}{16} \right) \right\}. \tag{3.6}$$

The volume flow rate being initial condition is utilized to obtain axial pressure gradient $\left(\frac{\partial p}{\partial z} \right)$ from [1, 14, 17, 24]:

$$Q = 2\pi \int_0^{h_z} r w dr.$$

From volume flow rate, pressure gradient $\left(\frac{\partial p}{\partial z} \right)$ is determined as:

$$\frac{\partial p}{\partial z} = 16 (Q/2\pi) \left(-\frac{1}{h_z^4} \right) - \beta \left[\left(\frac{512}{3} \right) (Q/2\pi)^2 \left(\frac{-1}{h_z^7} \right) + 256(Q/2\pi)^2 \left(\frac{1}{h_z^7} \right) \left(\frac{\partial h_z}{\partial z} \right) \right]. \tag{3.7}$$

The axial velocity (w) is evaluated by using Equation (3.7) in Equation (3.6). Wall shear stress (τ_w) is to be evaluated by using Equation (3.7) and equation (2.7) in Equation (2.8).

An exact solution for velocity is obtained from Equation (2.12) considering the boundary and initial condition as: $\frac{\partial w}{\partial r} = 0$ at $r = 0$; $w = 0$ at $r = h_z$ and $u = finite\ and\ constant$ and is reported in our earlier paper [26]. The final expressions are reproduced below.

$$\frac{\partial p}{\partial z} = 4(\beta u)^4 \ln \left(\frac{2\beta u}{h_z - 2\beta u} \right)^2 - 4\beta^3 u^3 h_z - \beta^2 u^2 h_z^2 - \frac{\beta u h_z^3}{3} - \frac{h_z^4}{8}. \tag{3.8}$$

Axial velocity is expressed as:

$$w = \frac{Q \left[\left(\frac{h_z^2 - r^2}{2} \right) + 2\beta u (h_z - r) - 2\beta^2 u^2 \ln \left(\frac{r - 2\beta u}{h_z - 2\beta u} \right)^2 \right]}{\pi \left[4(\beta u)^4 \ln \left(\frac{2\beta u}{h_z - 2\beta u} \right)^2 - 4\beta^3 u^3 h_z - \beta^2 u^2 h_z^2 - \frac{\beta u h_z^3}{3} - \frac{h_z^4}{8} \right]}. \tag{3.9}$$

The wall shear stress can be expressed as:

$$\tau_w = \frac{Q h_z^2}{(2\beta u - h_z) \left[\frac{h_z^4}{8} + \frac{\beta u h_z^3}{3} + \frac{\beta^2 u^2 h_z^2}{2} + 4\beta^3 u^3 h_z + 4(\beta u)^4 \ln \left(\frac{2\beta u - h_z}{2\beta u} \right)^2 \right]}. \tag{3.10}$$



Variation of axial velocity (w) with respect to radial distance (r) is computed using Equation (3.8) in Equation (3.9). For exact solution, Equation (3.10) is used to compute wall shear stress.

4. SOLUTION OF POWER LAW AND CASSON MODELS:

The z momentum equation in Equation (2.6) is integrated with respect to r and it becomes:
 $\tau_{rz} = \frac{\Delta p}{2l} r + \frac{k}{r}$, where k is constant of integration and $k = 0$ at $r = 0$, stress being finite. Further, equating with shear stress at wall it becomes:

$\tau_{rz} = \frac{\Delta p}{2l} r = \tau_w \frac{r}{h_z}$, where, τ_w is shear stress evaluated at wall.

Using Power Law constitutive relation, the velocity is obtained as:

$$w = \left(\frac{\tau_w}{m}\right)^{\frac{1}{n_p}} \frac{h_z}{\left(1 + \frac{1}{n_p}\right)} \left\{ 1 - \left(\frac{r}{h_z}\right)^{\left(1 + \frac{1}{n_p}\right)} \right\}. \tag{4.1}$$

Substituting Equation (4.1) in expression of volumetric flow rate: $Q = 2\pi \int_0^{h_z} r w dr$, the expression of velocity becomes:

$$w = \left(\frac{Q}{\pi h_z^2}\right) \frac{\left(3 + \frac{1}{n_p}\right)}{\left(1 + \frac{1}{n_p}\right)} \left\{ 1 - \left(\frac{r}{h_z}\right)^{\left(1 + \frac{1}{n_p}\right)} \right\}. \tag{4.2}$$

For Casson fluid [23]

Axial Velocity:

$$w = \left(\frac{\partial p}{\partial z}\right) \frac{(h_z)^2}{(4\mu)} \left[\frac{(r^2 - h_z^2)}{h_z^2} + \frac{1}{\left(\frac{\partial p}{\partial z}\right)} \left(\frac{4\tau_0}{h_z}\right) \left(\frac{r - h_z}{h_z}\right) - \sqrt{\frac{128\tau_0}{9\left(\frac{\partial p}{\partial z}\right)} \frac{(r^3 - h_z^3)}{h_z^3}} \right], \tag{4.3}$$

where,

$$\frac{\partial p}{\partial z} = - \left(\frac{128\tau_0}{49h_z} + \frac{8\mu Q}{\pi h_z^4} + \frac{64}{7h_z} \sqrt{\frac{\mu Q \tau_0}{\pi h_z^3}} \right). \tag{4.4}$$

The expression of axial velocity is obtained in Equation (3.6) for Reiner Rivlin fluid by Perturbation method. The results of same is compared with the results obtained from exact solution of Reiner Rivlin in Equation (3.9) and Equations (4.2) and Equation (4.3) for Casson constitutive relation.

5. NUMERICAL RESULTS AND DISCUSSION:

Computer codes are written in MATLAB to compute axial velocity (w) and wall shear stress (τ_w) substituting values of ratio of cross viscosity to viscosity (β), flow rate (Q) and stenotic wall radius (h_z). Stenotic wall radius (h_z) is computed using values of shape parameter (n), taper angle of artery (θ) and height of stenosis (δ).

A semi-analytical Perturbation solution for flow field for Reiner Rivlin is developed. Perturbation method employs ratio of cross viscosity to viscosity (β) as the perturbation parameter. Expression for axial velocity is obtained after considering up to first order of expansion, ignoring higher order terms. Axial velocity profiles with respect to radial distance obtained from Perturbation solution and exact solution are plotted in Figure 7. It is observed that the perturbation solution computes lower axial velocity with respect to r in the plug region. But as the radial distance increases, the both the solutions get closer. The root mean squared difference is also computed and the value is 0.0051. The axial velocity profile of Perturbation solution is relatively flatter near the centre compared to the profile obtained from exact solution. The squared difference between the axial velocity computed from exact solution and Perturbation solutions at different radial distance has been computed and is plotted in Figure 3. It is observed that the squared difference decreases sharply as r increases beyond some value. In Reiner Rivlin, ratio of cross viscosity to viscosity (β) term incorporates non-Newtonian character to the blood. As (β) increases the non-Newtonian character becomes relatively more significant. Considering ($\beta=0$), Newtonian flow field is recovered in both exact solution and



Perturbation solutions. For different (β) , the axial velocity profiles for Reiner Rivlin are plotted for exact solution and Perturbation solutions in Figure 4 and Figure 5 respectively. From the literature, it is suggested that in Newtonian fluid, the axial velocity profile exhibits parabolic trend. At $(\beta=0)$, values for Newtonian fluid is obtained where the axial velocity profile is parabolic. As (β) increases, the trend line deviates from the parabolic pattern. Higher (β) , higher is the axial velocity at the centre but shows a sharp fall with the increase in the values of r . Figure 6 shows the variation of mean squared difference of axial velocity obtained from exact solution and Perturbation solution with respect to (β) . It is observed that as the value of (β) increases the mean squared difference of axial velocity between exact solution and Perturbation solution increases. This is due to the fact that (β) is Perturbation parameter and therefore, it has significant effect on the computed values of axial velocity. The expressions of axial velocity have been deduced considering zeroth order and first order of (β) and all higher orders are neglected. At higher (β) , the effect of neglecting higher order of (β) results in higher mean squared difference relative to lower (β) . Therefore, Perturbation solution is relatively close to exact solution at low values of (β) as the Perturbation solution is (β) sensitive.

Figure 7 shows the variation of axial velocity with respect to radial distance for Reiner Rivlin and Power Law constitutive relations. It is observed that axial velocity profile for Reiner Rivlin fluid shows similar trend with respect to Power law for $n > 1$. For $n < 1$, the axial velocity profile is observed to be relatively blunt. Axial velocity profile of Reiner Rivlin at $(\beta = 0.3)$ fairly corresponds to the axial velocity profile for Power Law at $n = 1.2$. Therefore, it may be concluded that using Reiner Rivlin differential type model, flow field of blood under stenotic artery can be satisfactorily determined.

The variation of wall shear stress with respect to axial distance along the length of the stenosis for Reiner Rivlin is plotted in Figure 8. From Figure 8, it is seen that wall shear stress developed in case of Perturbation solution is higher than the wall shear stress obtained in exact solution. For symmetric stenosis, the wall shear stress profile obtained from exact solution is symmetric where as in case of Perturbation solution, wall shear stress profile is not symmetric. The variation of wall shear stress with respect to axial distance along the length of the stenosis for Power Law and Reiner Rivlin at $(\beta = 0.1)$ is plotted in Figure 8. Wall shear stress profiles for $m = 1$ and $n = 0.8, 1.0$ and 1.2 are plotted respectively. It may be noted that wall shear stress for Newtonian is obtained by taking $m = 1$ and $n = 1.0$ in Power Law model. From Figure 8, it is observed that similar to Reiner Rivlin exact solution, the wall shear stress profile in case of Power law and Newtonian is symmetric for symmetric stenosis. The wall shear stress profile of Reiner Rivlin shows significant similarity with profiles of Power law. Thus, the model for Reiner Rivlin is significantly appropriate in simulating flow field of blood in stenotic artery.

6. CONCLUSION

Mathematical models for axisymmetric blood flow through symmetric mild stenosis are worked out by the analytical and semi-analytical Perturbation methods. Blood flow is considered to obey Reiner-Rivlin fluid having an additional cross viscosity parameter. The exact solution and Perturbation solutions are obtained from the z-momentum equation in non-dimensional form. The expressions for the axial velocity and wall shear stress distribution along the length of the stenotic region are derived. The nature of variation of axial velocity and wall shear stress are studied by plotting graphs of the results obtained by exact solution and Perturbation solutions. Further, axial velocity profiles and wall shear stress profiles of Reiner Rivlin are compared with Newtonian and Power Law profiles. The main findings can be summarized as follows:

- (1) Axial velocity obtained from Perturbation solution is fairly close to the exact solution with a mean squared difference of 0.024 at $(\beta = 0.3)$. However, Perturbation solution yields higher axial velocity compared to exact solution.
- (2) At $(\beta = 0.3)$, the squared difference of axial velocity between exact solution and Perturbation solution becomes rapidly smaller as r increases.
- (3) The mean squared difference of axial velocity between exact solution and Perturbation solution increases as the ratio of cross viscosity to viscosity (β) increases. This happens because in Perturbation method higher order of β is ignored, that becomes relatively significant at high values of β .



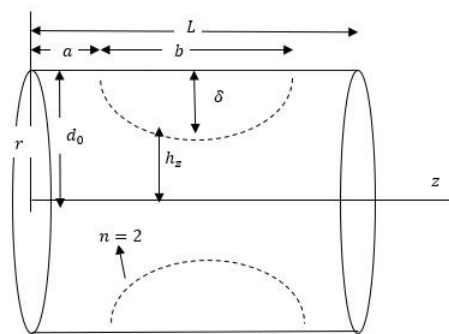


FIGURE 1. Schematic diagram of stenotic artery with co-ordinate system.

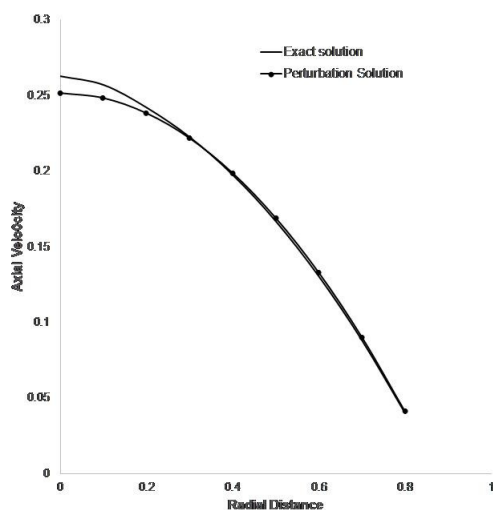


FIGURE 2. Variation of axial velocity with respect to Radial distance for Reiner Rivlin Constitutive Relation with Root Mean Squared Difference=0.0051. $n = 2, \delta = 0.125, s = 0.8, z = 0.5, Q = 0.3, u = 0.1,$ and $\beta = 0.3$.

- (4) Axial velocity profile of Reiner Rivlin has close similarity with axial velocity profiles obtained by taking different n in Power law constitutive relation. Axial velocity profile of Reiner Rivlin at $\beta = 0.3$ is fairly close to Power law at $n = 1.2$.
- (5) Wall shear stress profile of Reiner Rivlin shows striking similarity with profiles of Power Law and Newtonian. The profiles are symmetric in symmetric stenosis.
- (6) Wall shear stress profile obtained from Perturbation solution is found to be non-symmetric which is in contradiction to the accepted trend.

Therefore, it is concluded that considering Reiner Rivlin constitutive relation, the exact solution developed in the present paper can be satisfactorily utilised to simulate flow field of blood in stenosed artery.

7. THE FIGURES



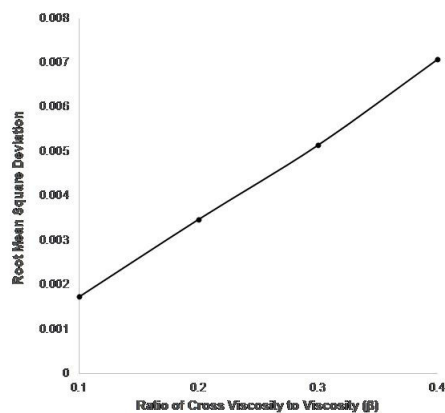


FIGURE 3. Root Mean squared difference between axial velocity computed from Exact and Perturbation Solution with respect to Ratio of Cross Viscosity to Viscosity for Reiner Rivlin Constitutive Relation. $n= 2, \delta= 0.125, s= 0.8, z= 0.5, Q= 0.3, u= 0.1$.

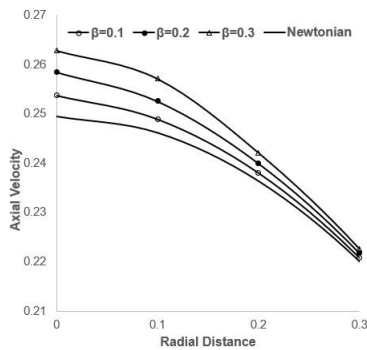


FIGURE 4. Axial velocity Profile with respect to Radial distance obtained from Exact solution for Reiner Rivlin and Newtonian Constitutive Relations. $n= 2, \delta= 0.125, s= 0.8, z= 0.5, Q= 0.3, u= 0.1$



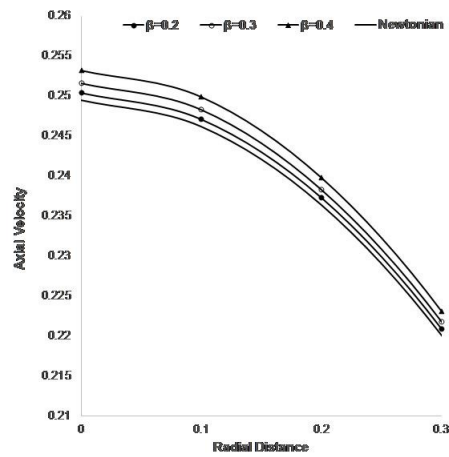


FIGURE 5. Axial velocity Profile with respect to Radial distance obtained from Perturbation solution for Reiner Rivlin and Newtonian Constitutive Relations. $n = 2, \delta = 0.125, s = 0.8, z = 0.5, Q = 0.3$.

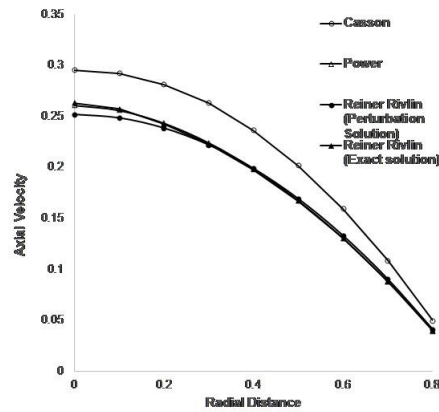


FIGURE 6. Variation of Axial velocity with respect to Radial distance for Reiner Rivlin, Casson and Power Law Constitutive Relations. $n = 2, \delta = 0.125, s = 0.8, z = 0.5, Q = 0.3, u = 0.1, n_p = 1.2, \tau_0 = 0.1, \mu_{ca} = 1.2, \beta = 0.3$.



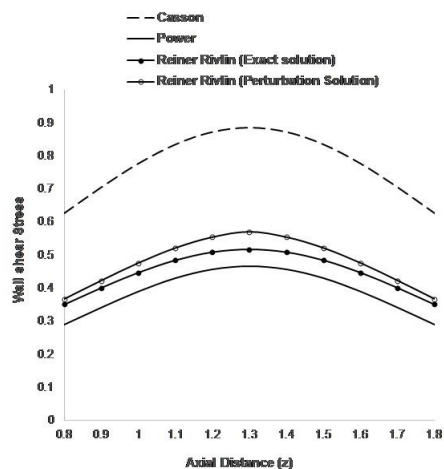


FIGURE 7. Variation of Wall Shear Stress with respect to axial distance along the length of Stenosis for Reiner Rivlin Constitutive Relation. $n=2, \delta=0.125, s=0.8, Q=0.3, u=0.1, m=2, n_p=1.2, \tau_0=0.1, \mu_{ca}=1.2, \beta=0.3$

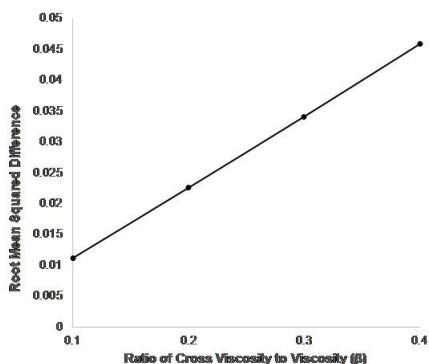


FIGURE 8. Variation of Root Mean Squared Difference in respect of Wall Shear Stress along the length of Stenosis with respect to Ratio of Cross Viscosity to Viscosity for Reiner Rivlin Constitutive Relation. $n=2, \delta=0.125, s=0.8, Q=0.3, u=0.1$



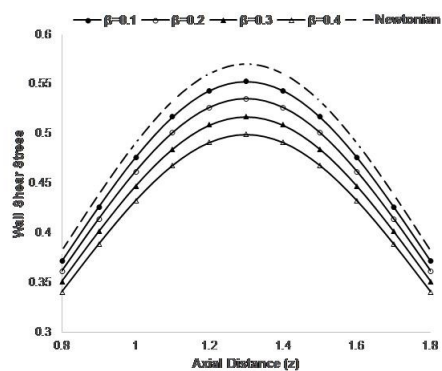


FIGURE 9. Variation of Wall Shear Stress with respect to axial distance along the length of Stenosis for Newtonian and Reiner Rivlin Constitutive Relations. $n=2, \delta=0.125, s=0.8, Q=0.3, u=0.1$.

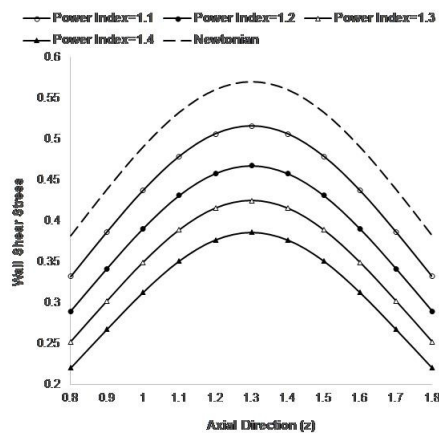


FIGURE 10. Variation of Wall Shear Stress with respect to axial distance along the length of Stenosis for Newtonian and Power Law at different Power index n_p . $\delta=0.125, s=0.8, Q=0.3, m=2.0$.



NOMENCLATURE

u : Non-dimensional Radial Component of velocity of flow
 \bar{u} : Radial Component of velocity of flow [ms^{-1}]
 u_0 : Averaged velocity on cross section of artery [ms^{-1}]
 w : Non-dimensional Axial Component of velocity of flow
 \bar{w} : Axial Component of velocity of flow [ms^{-1}]
 p : Non-dimensional Pressure
 \bar{p} : Pressure [Nm^{-2}]
 β : Ratio of cross-viscosity to viscosity
 Re : Reynold number
 a : Length of artery before the commencement of stenosis [m]
 b : Length of artery in stenotic region [m]
 L : Total length of artery [m]
 δ : Maximum height of stenosis [m]
 d_z : Radius of the tapered arterial segment [m]
 d_0 : Radius of non-tapered artery in non-stenotic region [m]
 $\tilde{\theta}$: Tapered angle of artery, [rad]
 ρ : Density of blood [kg m^{-3}]
 t : Non-dimensional time
 r : Non-dimensional radial distance
 z : Non-dimensional axial distance
 θ : Non-dimensional angular distance
 μ : Coefficient of Newtonian viscosity [$\text{kg m}^{-1}\text{s}^{-1}$]
 μ_c : Coefficient of Cross Viscosity [ms^{-1}].
 τ_{ij} : Stress tensor in non-dimensional form
 $\bar{\tau}_{ij}$: Stress tensor [Nm^{-2}]
 τ_0 : Yield Stress

REFERENCES

- [1] Z. Abbas, M. S. Shabbir, and N. Ali *Analysis of rheological properties of Herschel-Bulkley fluid for pulsating flow of blood in ω -shaped stenosed artery*, AIP Advances, 7 (2017), 1051123-1-12.
- [2] R. Ahmed, A. Farooki, R. Farooki, N. N. Hamadneh, M. F. Asad, I. Khan, M. Sajid, G. Bary, and M. F. S. Khan, *An Analytical Approach to Study the Blood Flow over a Nonlinear Tapering Stenosed Artery in Flow of Carreau Fluid Model*, Hindawi Complexity, Article ID 9921642, (2021).
- [3] N. S. Akbar, S. Nadeem, and Kh. S. Mekheimer, *Rheological properties of Reiner-Rivlin fluid model for blood flow through tapered artery with stenosis*, Journal of the Egyptian Mathematical Society, 24 (2016), 138–142.
- [4] N. S. Akbar and S. Nadeem, *Carreau fluid model for blood flow through a tapered artery with a stenosis*, Ain Shams Engineering Journal, 5 (2014), 1307–1316.
- [5] S. Akhtar, L. B. Mc Cash, N. Sohail, S. Saleem, and A. Issakhov, *Mechanics of non-Newtonian blood flow in an artery having multiple stenosis and electroosmotic effects*, Science Progress, 104(3) (2021), 1–15.
- [6] N. Antonova, *On Some Mathematical Models in Hemorheology*, Biotechnology & Biotechnological Equipment, 26(5) (2012), 3286-3291.
- [7] N. Dash and S. Singh, *Analytical Study of Non-Newtonian Reiner–Rivlin Model for Blood flow through Tapered Stenotic Artery*, Math. Biol. Bioinf., 15(2) (2020), 295-312.
- [8] Y. Egushi and T. Karino, *Measurement of rheologic property of blood by a falling-ball blood viscometer*, Ann Biomed Eng., 36(4) (2008), 545-553.
- [9] E. Fatahian, N. Kordani, and H. Fatahian, *A review on rheology of non-Newtonian properties of blood*, IIUM Engineering Journal, 19(1) (2018), 237-250.



- [10] A. K. Maiti, *Casson flow of blood through an arterial tube with overlapping stenosis*, IOSR Journal of Mathematics, *11*(6) (2015), 26-31.
- [11] M. A. Massoudi, *Generalization of Reiner's mathematical model for wet sand*, Mech. Res. Commun., *38* (2011), 378-381.
- [12] Kh. S. Mekheimer and M. A. El Kot, *The micropolar fluid model for blood flow through a tapered artery with a stenosis*, Acta Mech. Sin., *24* (2008), 637-644.
- [13] M. N. L. Narasimham, *On steady laminar flow of certain non-Newtonian liquids through an elastic tube*, Proceedings of Indian Academy of Sciences, Sec A, *43*(2) (1956), 237-246.
- [14] G. Neeraja, P. A. Dinesh, K. Vidya, and C. S. K. Raju, *Peripheral layer viscosity on the stenotic blood vessels for Herschel-Bulkley fluid model*, Informatics in Medicine Unlocked, *9* (2017), 161-165.
- [15] S. O'Callaghan, M. Walsh, and T. Mc Gloughlin, *Numerical modelling of Newtonian and non-Newtonian representation of blood in a distal end-to-side vascular bypass graft anastomosis*, Med. Eng. Phys., *28* (2006), 70-74.
- [16] S. L. Rathna and P. L. Bhatnagar, *Weissenberg and Merrington effects in non-Newtonian fluids*, Jl. of Indian Institute of Science, *45*(2) (1962), 57-82.
- [17] R. Revellin, F. Rousset, D. Baud, and J. Bonjour, *Extension of Murray's law using a non-Newtonian model of blood flow*, Theoretical Biology and Medical Modelling, *6*(9) (2009), 1-9.
- [18] S. Sapna, *Analysis of non-Newtonian fluid flow in a stenosed artery*, International Journal of Physical Sciences, *4*(11) (2009), 663-671.
- [19] S. Sreenadh, A. R. Pallavi, and B. H. Satyanarayana, *Flow of a Casson fluid through an inclined tube of non-uniform cross section with multiple stenoses*, Adv Appl Sci Res., *2*(5) (2011), 340-349.
- [20] B. Thomas and K. S. Suman, *Blood Flow in Human Arterial System-A Review*, Procedia Technology, *24* (2016), 339-346.
- [21] G. B. Thurston, *Erythrocyte Rigidity as a Factor in Blood Rheology: Viscoelastic Dilatancy*, Journal of Rheology, *23*(6) (2000), 703.
- [22] G. B. Thurston and N. M. Henderson, *Effects of flow geometry on blood viscoelasticity*. Biorheology., *43*(6) (2006), 729-746.
- [23] J. Venkatesan, D. S. Sankar, K. Hemalatha, and Y. Yatim, *Mathematical Analysis of Casson Fluid Model for Blood Rheology in Stenosed Narrow Arteries*, Journal of Applied Mathematics., Article ID 583809, (2013).
- [24] V. K. Verma, *Study of Non-Newtonian Herschel-Bulkley Model through Stenosed Arteries*, International Journal of Mathematics and its Application, *4*(1-B) (2016), 105-111.
- [25] D. F. Young, *Fluid mechanics of arterial stenosis*, J Biomech Eng., *101* (1979), 157-175.
- [26] F. Yilmaz and M. Y. Gundogdu, *A critical review on blood flow in large arteries; relevance to blood rheology, viscosity models, and physiologic conditions.*, Korea-Australia Rheology Journal, *20*(4) (2008), 197-211.

